JOURNAL OF COMPUTATIONAL PHYSICS 28, 357–375 (1978)

Numerical Solution of the Dynamic Equation for Particulate Systems

FRED GELBARD AND JOHN H. SEINFELD

Department of Chemical Engineering, California Institute of Technology, Pasadena, California 91125

Received June 16, 1977; revised September 26, 1977

The method of collocation using two finite element techniques is applied to the solution of the general population balance equation for particulate systems. Numerical solutions by both techniques are obtained in six cases for which analytical or asymptotic solutions are available. Errors associated with solving the equation on a finite particle size domain are analyzed. The results indicate that, for simulating particulate system dynamics, both techniques are highly accurate and efficient.

1. INTRODUCTION

The state of a spatially and chemically homogeneous particulate system is described by its size distribution density function, $n_v(v, t)$, where $n_v(v, t)\, dv$ is the number of particles per unit volume of fluid having volumes in the range v to $v + dv$. The dynamics of such a system in which individual particles may grow through accretion of material from the fluid phase (or shrink by loss of material) and in which particles may collide and coagulate are described by the general particulate balance equation [1, 2]

$$\frac{\partial n_v(v, t)}{\partial t} = -\frac{\partial}{\partial v}\left[I_v(v, t)\, n_v(v, t)\right] + \int_0^{v/2} \beta_v(v - \tilde{v}, \tilde{v})\, n_v(v - \tilde{v}, t)\, n_v(\tilde{v}, t)\, d\tilde{v} - n_v(v, t) \int_0^{\infty} \beta_v(v, \tilde{v})\, n_v(\tilde{v}, t)\, d\tilde{v} + S_v[n_v(v, t), v, t] \tag{1}$$

where $I_v(v, t) = dv/dt$, the rate of change of the volume of a particle of volume v by transfer of material between the particle and the fluid phase, $\beta_v(v, \tilde{v})$ is the coagulation coefficient for particles of volumes v and $\tilde{v}$, and S_v is the net rate of addition of fresh particles into the system. The initial and boundary conditions required for (1) are generally stated as

$$n_v(v, 0) = n_{v_0}(v) \tag{2}$$

0021-9991/78/0283–0357$02.00/0

and

$$n_v(0, t) = 0, \tag{3}$$

respectively. (The latter condition indicates that there are no particles of zero size.)

The first term on the right-hand side of (1) represents the rate of growth of particles by transfer of material to individual particles. The second term represents the rate of accumulation of particles in the size range $(v, v + dv)$ by collision of two particles of volumes $v - \tilde{v}$ and $\tilde{v}$ to form a particle of volume v (assuming conservation of volume during coagulation). The third term represents the rate of loss of particles in the size range $(v, v + dv)$ by collision with all other particles. The last term represents all particle sources and sinks. Equation (1) arises in a wide variety of physical contexts, such as colloid chemistry, atmospheric aerosol dynamics, crystallization kinetics, and biological population dynamics.

Equation (1) can also be written in terms of particle diameter D (assuming spherical particles),

$$\begin{aligned}\frac{\partial n_D(D, t)}{\partial t} = &- \frac{\partial}{\partial D}\left[I_D(D, t)\, n_D(D, t)\right] \\ &+ D^2 \int_0^{D/2^{1/3}} \beta_D(\psi, \tilde{D})\, n_D(\psi, t)\, n_D(\tilde{D}, t)\, \frac{d\tilde{D}}{\psi^2} \\ &- n_D(D, t) \int_0^{\infty} \beta_D(D, \tilde{D})\, n_D(\tilde{D}, t)\, d\tilde{D} \\ &+ S_D[n_D(D, t), D, t]\end{aligned} \tag{4}$$

where $n_D(D, t) = (\pi D^2/2) n_v(v, t)$, $\psi = (D^3 - \tilde{D}^3)^{1/3}$, and $I_D = dD/dt$.

In spite of the great importance of (1) and (4) to particulate system dynamics, solutions have been difficult to obtain. Analytical solutions are available only for a few simple forms of the initial conditions, $\beta_v(v, \tilde{v})$, $I_v(v, t)$, and $S_v[n(v, t), v, t]$ [2–5]. Numerical solutions have been reported [6–16] but the optimum method for solving (1) has not been determined.

In this work we report on two collocation techniques used to solve the general dynamic equation. In Section 2 we discuss the proper scaling of the equation, in Section 3 we develop both methods, and in Section 4 we describe the results of applying both methods to several test problems for which analytical or asymptotic solutions are available.

2. Scaling of the Equations

Equations (1) and (4) must be rescaled to a finite domain prior to numerical solution. We select a dimensionless finite particle size domain scaled from zero to one. Let us denote v_a, v_b, and D_a, D_b as the chosen lower and upper limits on the volume and diameter, respectively, that will be employed in the numerical solution. Two

possible transformations to a finite particle size domain (D_a, D_b) are linear and logarithmic [13],

$$u = (D - D_a)/(D_b - D_a) \qquad \text{or} \qquad u = (v - v_a)/(v_b - v_a) \tag{5}$$

and

$$w = \frac{\ln(D/D_a)}{\ln(D_b/D_a)} = \frac{\ln(v/v_a)}{\ln(v_b/v_a)}. \tag{6}$$

For the representation of real systems, the logarithmic transformation (6) is preferred over the linear transformation (5). Generally, the larger number of particles occur in the smallest size range, and (6) more effectively expands that region. If significant effects occur equally over the entire particle size range, then a linear transformation (5) is preferred. The use of a finite particle size domain introduces errors in that the general dynamic equation is based on an infinite particle size domain. For an actual particulate system, however, there are usually upper and lower bounds on the sizes of the particles that exist. In theory, D_a should be chosen as the diameter of the smallest existing particle. (Although the general equations are written as if there exists a continuous spectrum of sizes down to zero, there is actually a lower cutoff in a real system.) D_b should be chosen large enough to include nearly all the particles in the system, yet small enough so that the region of major dynamic activity is not obscured. We will discuss the choice of D_a and D_b subsequently.

The analytical solutions of (1) currently available are based on rather idealized forms of the initial conditions, β_v, I_v, and S_v [2–5]. For that reason, these solutions do not correspond directly to realistic physical conditions. Nevertheless, the use of available analytical solutions represents the only unambiguous way to ascertain the accuracy of the numerical solutions. Thus, in this work we will concentrate on obtaining numerical solutions for those cases for which analytical solutions are available.

Since aerosol data are usually given in terms of particle diameter, and the logarithmic transformation (6) has the same form for either particle volume or diameter, we choose to develop the numerical solution in terms of particle diameter.

Using (6), (4) becomes

$$\begin{aligned}\frac{\partial m(w,t)}{\partial t} = &- \frac{\partial}{\partial w}[I(w,t)\, m(w,t)] \\ &+ \zeta^{3w} \int_0^{w-\ln 2/3\ln\zeta} \beta(x,z)\, m(x,t)\, m(z,t) \frac{dz}{\zeta^{3w} - \zeta^{3z}} \\ &- m(w,t) \int_0^1 \beta(w,z)\, m(z,t)\, dz + S[m(w,t), w, t]\end{aligned} \tag{7}$$

where $I = dw/dt$ and

$$\begin{aligned} x &= \ln(\zeta^{3w} - \zeta^{3z})/3 \ln \zeta, \\ \zeta &= D_b/D_a, \end{aligned} \tag{8}$$

and

$$m(w, t) = D \ln \zeta n_D(D, t), \tag{9}$$

$$S = D_a \zeta^w \ln \zeta S_D . \tag{10}$$

From (9), we can relate $m(w, t)$ and $n_v(v, t)$ as follows:

$$n_v(v, t) = (2/\pi \ln \zeta D^3) m(w, t). \tag{11}$$

3. Collocation on Finite Elements

The most promising class of methods for solving (7) is that based on the methods of weighted residuals, in which the form of the solution is assumed in terms of a complete set of functions (generally polynomials) and substituted into the governing equation [17, 18]. To produce equations for the unknown coefficients of the expansion, the equation is multiplied by a weight factor, which is dependent on the method used, and integrated over the domain of interest. Among all the commonly used methods of weighted residuals, such as collocation, the Galerkin method and the method of moments, only collocation does not require extensive integral evaluations. Therefore, collocation emerges as the most attractive method of weighted residuals for (7).

In the traditional application of collocation a finite expansion of order $\overline{M}$ is forced to satisfy the differential equation at $\overline{M} + 1$ predetermined collocation points, hence the residual is zero at these points. If the expansion satisfies the differential equation at all points in the region and at the boundary, then the expansion is by definition a representation of the exact solution. However, due to the large variations in magnitude of $m(w, t)$ a single high-order polynomial fit is not feasible. Therefore the finite element technique combined with collocation [19, 20] represents a promising approach.

For both finite element techniques the domain of the independent variable is divided into elements within which the dependent variable is represented by a polynomial, often a cubic. At the grid points between elements the distributions and their derivatives are forced to be continuous. If the second derivative is forced to be continuous and collocation points are also taken at the grid points, then the finite element fit is actually a cubic spline. If within each element the independent variable is rescaled from 0 to 1 to avoid roundoff errors, and collocation points are taken as the roots of the shifted Legendre polynomial, then we have what has been called orthogonal collocation on finite elements [20]. Since cubic splines are described in the literature [21, 22], and they were originally reported in [16] only orthogonal collocation on finite elements will be described here. Because it is easier to write the code in terms of the distribution at the collocation points and not the expansion coefficients, the solution technique will be given in terms of the distribution at the collocation points.

Dividing the distribution, $m(w, t)$ into M elements and using a cubic polynomial in each element results in the following representation of $m(w, t)$ in the ith element,

$$m(w, t) = A_{i,1}(t) + A_{i,2}(t) y_i + A_{i,3}(t) y_i^2 + A_{i,4}(t) y_i^3, \qquad i = 1, 2, \ldots, M, \tag{12}$$

where $A_{i,j}$ is the jth coefficient of the ith element, and $y_i = (w - w_{i-1})/(w_i - w_{i-1})$ for $w_{i-1} < w \leqslant w_i$. Imposing the condition of continuity of $m(w, t)$ and its first derivative at the grid points gives

$$A_{i,1} + A_{i,2} + A_{i,3} + A_{i,4} = A_{i+1,1}, \tag{13}$$

$$A_{i,2} + 2A_{i,3} + 3A_{i,4} = \frac{(w_i - w_{i-1})}{(w_{i+1} - w_i)} A_{i+1,2}. \tag{14}$$

At each collocation point η within each element we have

$$A_{i,1} + \eta A_{i,2} + \eta^2 A_{i,3} + \eta^3 A_{i,4} = B_{i,k} \tag{15}$$

and where $B_{i,k}$ represents the distribution, $m(w, t)$ at the kth collocation point in the ith element and $w = \eta(w_i - w_{i-1}) + w_{i-1}$. Using (13) and (14) we can derive the following set of $2M + 2$ linear algebraic equations for $A_{i,j}$

$$\begin{aligned}
&(1 - 3\eta_k^2 + 2\eta_k^3) A_{i,1} + (\eta_k - 2\eta_k^2 + \eta_k^3) A_{i,2} + (3\eta_k^2 - 2\eta_k^3) A_{i+1,1} \\
&\frac{(w_i - w_{i-1})}{(w_{i+1} - w_i)} (\eta_k^3 - \eta_k^2) A_{i+1,2} = B_{i,k}, \qquad i = 2,\ldots, M-1, \quad k = 1, 2, \\
&\qquad\qquad i = 1, \quad k = 1, 2, 3;
\end{aligned} \tag{16}$$

and

$$A_{M,1} + \eta_k A_{M,2} + \eta_k^2 A_{M,3} + \eta_k^3 A_{M,4} = B_{M,k}, \qquad k = 1, 2, 3. \tag{17}$$

When placed in conventional matrix form, (16) and (17) lead to a banded matrix of bandwidth 7 that can be inverted easily. Since the elements of the matrix are time independent, elimination need only be carried out once.

The final consideration is the location of the finite elements. In [20] it is suggested that the elements be located to minimize the residual. Although this is a reasonable criterion, it would require a costly iterative procedure in the present application. Without any prior knowledge of the behavior of $m(w, t)$, the elements were equally spaced in w, or in terms of a dimensionless diameter.

4. Numerical Implementation

We will consider the exponential initial volume distribution

$$n_{v_0}(v) = (N_0/v_0)\, e^{-\bar{v}} \tag{18}$$

where N_0 is the total initial number of particles, v_0 is the mean initial volume, and $\bar{v} = v/v_0$.

Because the mechanism of coagulation poses the greatest numerical difficulty, we will first consider the solution of (7) in the absence of growth and sources. In this case

we will show the effect of using a finite particle size domain by studying two different collision mechanisms, $\beta_v = \beta_0$ and $\beta_v = \beta_1(v + \tilde{v})$. As mentioned previously, in actual particulate systems an upper limit to the particle size exists because of removal mechanisms, such as sedimentation or deposition. Therefore, the effects on the

TABLE I

Summary of Cases Considered of the General Dynamic Equation for Particulate Systems[a]

$$\frac{\partial n_v}{\partial t} = -\frac{\partial}{\partial v}(I_v n_v) + \int_0^{v/2} \beta_v(v - \tilde{v}, \tilde{v}) n_v(v - \tilde{v}, t) n_v(\tilde{v}, t)\, d\tilde{v} - n_v(v, t) \int_0^{\infty} \beta_v(v, \tilde{v}) n(\tilde{v}, t)\, d\tilde{v} + S_v(n_v, v, t)$$

Case	$\beta_v(v, \tilde{v})$	$I_v(v, t)$	$S_v(n_v, v, t)$	Analytical solutions	Domain $[\tilde{v}_a, \tilde{v}_b]$
1	β_0	0	0	[4]	$[10^{-9}, 27]$
2	β_0	0	0	[4]	$[10^{-9}, 64]$
3	$\beta_1(v + \tilde{v})$	0	0	[3, 4]	$[10^{-9}, 27]$
4	$\beta_1(v + \tilde{v})$	0	$-R_0 n_v$	[5]	$[10^{-9}, 27]$
5	β_0	σv	0	[2]	$[10^{-9}, 27]$
6	β_0	0	$(S_0 e^{-v/v^*}/v^*) - R_0 n_v$	[5]	$[10^{-9}, 27]$

[a] R_0, S_0, and σ are constant.

TABLE II

Dimensionless Groups Associated with the General Dynamic Equation for Particulate Systems

Group	Interpretation
$\tau = N_0\beta_0 t$ (Cases 1, 2, 5, 6) $= N_0 v_0 \beta_1 t$ (Cases 3, 4)	Dimensionless time
$\Lambda = \sigma/N_0\beta_0$ (Case 5)	Condensation rate / Coagulation rate
$\theta = R_0/N_0 v_0 \beta_1$ (Case 4) $= R_0/N_0\beta_0$ (Case 6)	Removal rate / Coagulation rate
$\Omega = S_0/N_0^2\beta_0$ (Case 6)	Source rate / Coagulation rate

distribution of a first-order removal mechanism will be studied. Then, the effect of simultaneous coagulation and growth will be studied. Finally, the numerical solution will be compared to an asymptotic solution for a system undergoing simultaneous coagulation and removal with a constant particle source. The cases considered are summarized in Table I.

Particulate size distributions can be represented in a variety of ways. When the predominant number of particles occurs in the small size regime, we select a representation that expands the lower end of the spectrum. In such a case the distribution is usually represented versus a logarithmic size coordinate, e.g., (6). When representing the analytical solutions to the cases listed in Table I, however, it is most convenient to use, as the independent variable, $\bar{D}$ and, as the dependent variable, $\bar{n}_{\bar{D}}(\bar{D}, t)/N_0$, where $\bar{D} = D/D_0$, $D_0 = (6v_0/\pi)^{1/3}$, and $\bar{n}_{\bar{D}}(\bar{D}, t) = D_0 n_D(D, t)$.

All solutions will be expressed in terms of dimensionless groups, defined for each case in Table II. Since all cases include coagulation, other mechanisms such as growth, removal, and sources will be expressed in terms of dimensionless groups scaled to coagulation. Although the definition of the dimensionless time τ varies depending on the coagulation mechanisms, for comparison purposes the same values of τ will be used in each case for which we present solutions. For convenience Λ, θ, and Ω will always be assumed to be unity. All analytical solutions will be shown as solid lines, and all numerical solutions will be represented by discrete points. Since both finite element techniques gave similar results both techniques are implied when numerical solutions are reported. The analytical solutions are given in Table III.

TABLE III

Analytical Solutions to (1) for Initial Distribution (18)

Case	β_v	I_v	S_v	$n_v(v, t)$	Reference
1, 2	β_0	0	0	$\dfrac{4N_0}{v_0(\tau+2)^2}\exp\left(-\dfrac{2\bar{v}}{\tau+2}\right)$	[4]
3[a]	$\beta_1(v+\bar{v})$	0	0	$\dfrac{N_0(1-T)}{v\,T^{1/2}}\exp(-(1+T)\bar{v})\,I_1(2\bar{v}\,T^{1/2})$	[3, 4]
4[b]	$\beta_1(v+\bar{v})$	0	$-R_0 n_v$	$\dfrac{N_0\hat{T}\exp\left(\dfrac{\hat{T}-1}{\theta}\right)}{v_0\,g^{1/2}\bar{v}}\exp\left(-(1+g)\bar{v}\right)I_1(2g^{1/2}\bar{v})$	[5]
5	β_0	σv	0	$\dfrac{4N_0}{v_0(\tau+2)^2}\exp\left(-\dfrac{2\bar{v}}{\tau+2}\exp(-\Lambda\tau)-\Lambda\tau\right)$	[2]

[a] $T = 1 - e^{-\tau}$, I_1, is the modified Bessel function of the first kind of order one.

[b] $g(\hat{T}) = 1 - \exp((\hat{T}-1)/\theta)$, $\hat{T} = \exp(-\theta\tau)$.

TABLE IV

Analytical Expressions for the Finite Domain Errors[a]

Case	$M_0(t)$	$M_1(t)$
1, 2	$\exp\left(-\frac{2\bar{v}}{\tau+2}\right)$	$\exp\left(-\frac{2\bar{v}}{\tau+2}\right)\left(\frac{2\bar{v}}{\tau+2}+1\right)$
3	$\sum_{k=0}^{\infty}\frac{(2k)!T^k}{k!(k+1)!}e^{-(1+T)\bar{v}}\sum_{r=0}^{2k}\frac{\bar{v}^{2k-r}}{(2k-r)!(1+T)^{r+1}}$	$(1-T)\sum_{k=0}^{\infty}\frac{(2k+1)!T^k}{k!(k+1)!}e^{-(1+T)\bar{v}}\sum_{r=0}^{2k+1}\frac{\bar{v}^{2k+1-r}}{(2k+1-r)!(1+T)^{r+1}}$
4	$\sum_{k=0}^{\infty}\frac{(2k)!g^k}{k!(k+1)!}\exp[-\bar{v}(1+g)]\sum_{r=0}^{2k}\frac{\bar{v}^{2k-r}}{(2k-r)!(1+g)^{r+1}}$	$\exp\left(\frac{\hat{T}-1}{\theta}\right)\sum_{k=0}^{\infty}\frac{(2k+1)!g^k}{k!(k+1)!}\exp(-\bar{v}(1+g))\sum_{r=0}^{2k+1}\frac{\bar{v}^{2k+1-r}}{(2k+1-r)!(1+g)^{r+1}}$
5	$\exp\left(-\frac{2\bar{v}}{\tau+2}\exp(-\Lambda\tau)\right)$	$\exp\left(-\frac{2\bar{v}}{\tau+2}\exp(-\Lambda\tau)\right)\left(\frac{2\bar{v}}{\tau+2}\exp(-\Lambda\tau)+1\right)$

[a] Each expression is to be evaluated at $\bar{v}_a$ minus its value at $\bar{v}_b$ ($\bar{v}_a = \bar{D}_a{}^3$ and $\bar{v}_b = D_b{}^3$).

4.1. *Finite Domain Error*

A major consideration in numerically solving an equation described over an infinite domain is the error incurred by the solution on a finite domain. To evaluate this so-called "finite-domain error," the fractions of the total number and volume of particles

TABLE V

Finite Domain Errors for Cases 1–5

Case	τ	M_0	M_1
1	1.0	1.00	1.00
	3.0	1.00	1.00
	5.0	1.00	0.996
	7.0	0.998	0.983
	10.0	0.989	0.939
	20.0	0.914	0.703
2	5.0	1.00	1.00
	10.0	1.00	1.00
	20.0	0.997	0.980
	30.0	0.982	0.908
	50.0	0.915	0.705
3	0.5	0.999	0.988
	1.0	0.983	0.776
	1.5	0.950	0.483
	2.0	0.921	0.283
	3.0	0.887	0.0979
	1.0	0.998	0.959
	2.0	0.990	0.856
	3.0	0.986	0.806
	5.0	0.983	0.780
	7.0	0.983	0.776
	10.0	0.983	0.776
5	1.0	0.999	0.990
	1.5	0.968	0.858
	2.0	0.839	0.545
	2.5	0.627	0.259
	3.0	0.416	0.102

contained in the finite computational domain can be determined based on the analytical solutions. Thus,

$$M_0(t) = \int_{v_a}^{v_b} n_v(v, t)\, dv \Big/ \int_0^{\infty} n_v(v, t)\, dv \tag{19}$$

and

$$M_1(t) = \int_{v_a}^{v_b} v n_v(v, t)\, dv \Big/ \int_0^{\infty} v n_v(v, t)\, dv \tag{20}$$

represent these two fractions. Obviously, we desire to select v_a and v_b such that M_0 and M_1 do not differ appreciably from unity but not so close to 0 and ∞, respectively, that the computational requirements are excessive. Due to the processes of coagulation and particle growth, larger particles are continually being formed. Thus, by using any finite domain, M_0 and M_1 must eventually decrease from unity. The time for

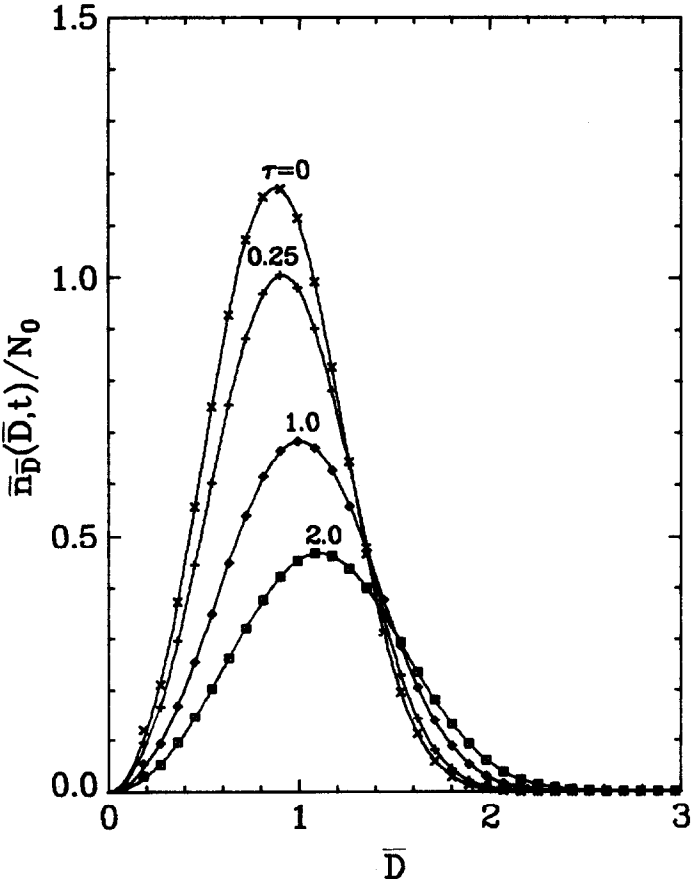

FIG. 1. Particle size spectra. $\beta_v = \beta_0$ and $\tau = N_0\beta_0 t$.

which M_0 and M_1 differ significantly from unity can be delayed by extending the domain at the expense of increased computational requirements.

It is important to note that (19) and (20) are evaluated based on the exact solution and therefore represent only the theoretical errors commited through the use of a finite computational domain. It is also important to distinguish the finite domain errors from errors usually associated with numerical solutions, in that regardless of the numerical method or its accuracy, there will be an error incurred merely because the computation is carried out on a finite rather than an infinite domain. Due to the nature of (1), particles within any finite computational domain interact with particles outside the computational domain. Hence, as more particles form outside the computational domain, unavoidable errors are introduced into the distribution within the computational domain. Therefore, all mechanisms which form particles rapidly at the upper end of the size spectrum can lead to errors within the computational

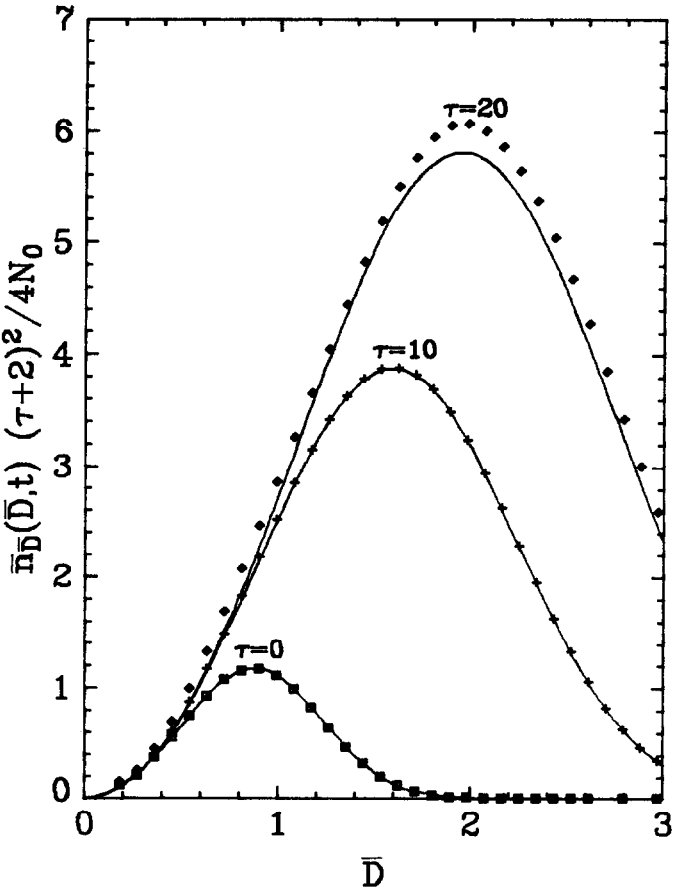

FIG. 2. Particle size spectra. $\beta_v = \beta_0$ and $\tau = N_0\beta_0 t$.

domain. For the cases given in Table III the analytical expressions for M_0 and M_1 are given in Table IV. Table V lists the finite domain errors for cases 1 to 5.

4.2. *Numerical Results*

The numerical and exact results for case 1 are shown in Fig. 1. Using equally spaced elements in $\bar{D}$, (7) was solved numerically by both methods of Section 3. Excellent agreement between the numerical and exact solutions was obtained. From Table V we see that for the times considered in Fig. 1 the finite domain errors are negligible. In fact, up to $\tau = 10$, no significant finite domain errors can be anticipated.

In order to demonstrate both the accuracy of both techniques for long dimensionless times and the effect of the finite domain error, case 1 was solved to $\tau = 20$. For the same domain as that in Fig. 1 Table V indicates that this domain will lead to a substantial finite domain error. By multiplying the distribution by $(\tau + 2)^2/4$, so as to emphasize the long-time behavior of the solution, Fig. 2 shows the numerical

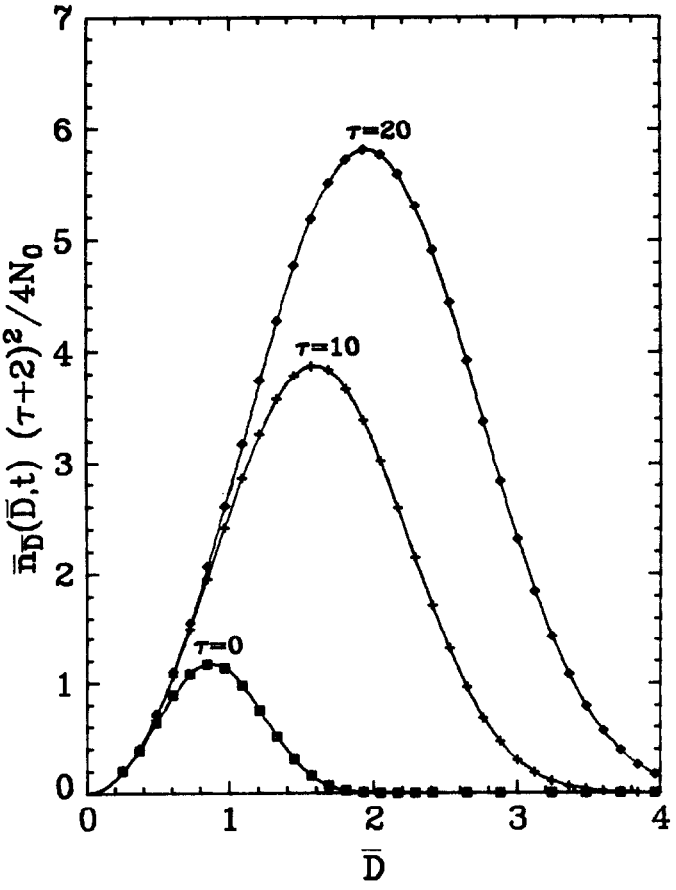

FIG. 3. Particle size spectra. $\beta_v = \beta_0$ and $\tau = N_0\beta_0 t$.

solution for $\bar{D}_b = 3.0$. At long times the numerical solution lies above the exact solution since the numerical solution does not account for collisions between particles inside the domain $[\bar{D}_a, \bar{D}_b]$ with those larger than $\bar{D}_b$. By increasing the computational domain, the finite domain errors are reduced, and hence an accurate solution can be obtained. From Table V for case 2 we see that if $\bar{D}_b$ is extended to 4.0 the finite domain errors are negligible for $\tau \leqslant 20$. As expected, Fig. 3 shows the numerical solution in excellent agreement with the exact solution when $\bar{D}_b = 4.0$.

Figure 4 shows exact and numerical solutions for case 3. Consistent with Table V, we see that as τ increases the deviation between the two solutions increases. The finite domain error is considerably more serious in case 3 than in case 1 because in case 3, β_v increases as the size of either particle increases, whereas in case 1, β_v is constant. Consequently, the shift of the spectrum to larger particle sizes is more rapid in case 3 at comparable values of the dimensionless time τ. At short times, $\tau < 1$, the numerical

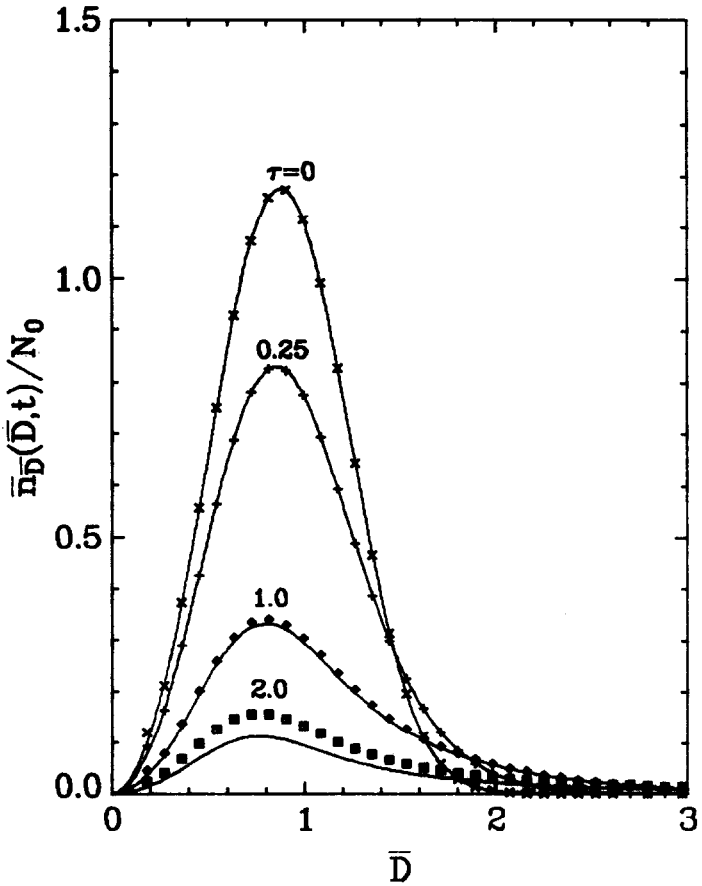

FIG. 4. Particle size spectra. $\beta_v = \beta_1(v + \bar{v})$ and $\tau = N_0\beta_1\nu_0 t$.

and exact solutions are very close. For longer times the numerical solution lies above the exact solution as in Fig. 2 for case 1. We can of course reduce the error by extending the computational domain. However, as mentioned previously, in most particulate systems removal mechanisms are present. Therefore, in order to study the effect of removal on the finite domain error in case 4 we consider $\beta_v = \beta_1(v + \tilde{v})$, $S_v = -R_0 n_v(v, t)$. From Table V we see a substantial decrease in the finite domain error with the addition of a first-order removal mechanism. Since there are fewer particles greater than $\bar{v}_b$ in case 4 as compared to case 3, the effect of coagulation of particles within the domain with particles outside the domain is negligible. Hence, Fig. 5 shows excellent agreement between the exact and numerical solutions.

Case 5 includes both coagulation and particle growth. Particle growth does not change the total number of particles; however, since only a finite domain is used in the numerical solution, particles will be artificially lost when they grow beyond the computational domain. From Table V we see that even greater finite domain errors

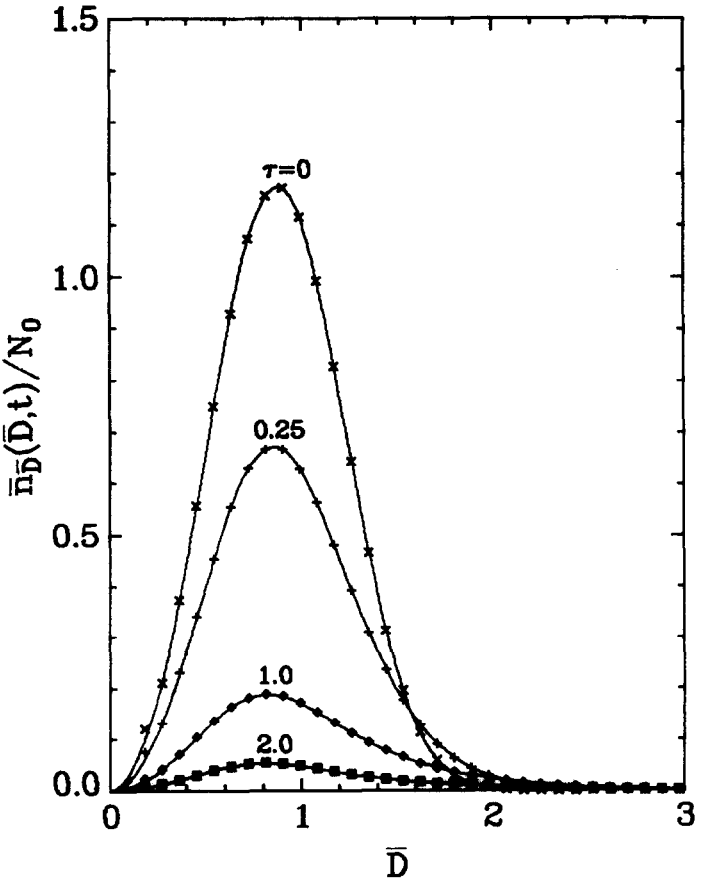

FIG. 5. Particle size spectra. $\beta_v = \beta_1(v + \tilde{v})$, $S_v = -R_0 n_v(v, t)$, $\tau = N_0\beta_1\nu_0 t$, and $\theta = R_0/\beta_1 N_0 \nu_0 = 1$.

in $M_0(t)$ exist for this case than for case 1. We see that particle growth is responsible for the additional error. Since the growth is independent of the distribution at any point in the domain, even for an infinite domain, the finite-domain errors shown in Table V do not lead to significant errors in the numerical solution. Thus, even though a substantial number of particles has been excluded, excellent agreement between the numerical and analytical solutions is still obtained, as shown in Fig. 6.

In case 6, $\beta_v = \beta_0$ and $S_v = (S_0/v^*) \exp(-v/v^*) - R_0 n_v$, where v^* is a measure of the range of particle volumes over which particles are being generated. For initial distribution (18) only an asymptotic solution for the large particle size end of the spectrum is available [5]. Since the exact solution is not available, only the total number and volume of particles can be calculated for an infinite domain. Integrating (1) over v from 0 to ∞ leads to the following equation for $N(t)$, the ratio of the number of particles present at time t to the initial number of particles,

$$dN/d\tau = -\tfrac{1}{2}N^2 - \theta N + \Omega \tag{21}$$

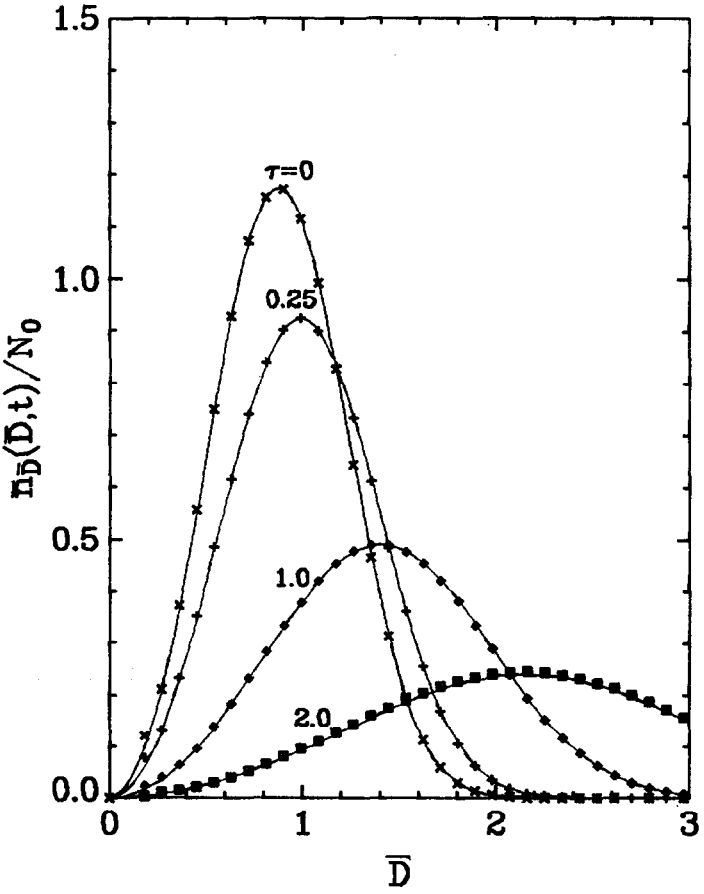

FIG. 6. Particle size spectra. $\beta_v = \beta_0$, $I_v = \sigma v$, $\tau = N_0\beta_0 t$, and $A = \sigma/N_0\beta_0 = 1$.

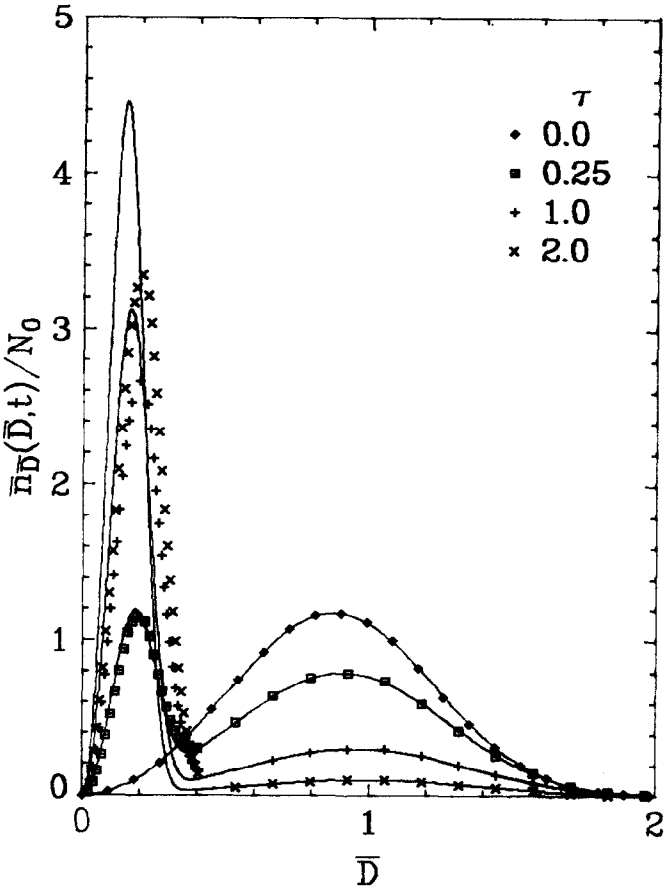

FIG. 7. Particle size spectra. $\beta_v = \beta_0$, $S_v = S_0/v^* \exp(-v/v^*) - R_0 n_v(v, t)$, $\tau = N_0\beta_0 t$, $\theta = R_0/\beta_0 N_0 = 1$, $\Omega = S_0/\beta_0 N_0^2 = 1$, and $\Delta = v^*/v_0 = 0.01$. (Computations were carried out on $\bar{D} = [0.001, 3.0]$. Only the region $\bar{D} = [0.001, 2.0]$ is shown.)

where

$$N(t) = \frac{1}{N_0} \int_0^\infty n_v(v, t)\, dv. \tag{22}$$

Similarly, the ratio V of the total volume of particles at any time t to the initial volume of particles is described by

$$dV/d\tau = -\theta V + \Delta\Omega \tag{23}$$

where $\Delta = v^*/v_0$ and

$$V(t) = \frac{1}{N_0 v_0} \int_0^\infty v n_v(v, t)\, dv. \tag{24}$$

Solving (21) and (23) yields

$$N(t) = \frac{r_1 - r_2\left(\frac{1 - r_1}{1 - r_2}\right)\exp\left(\frac{(r_2 - r_1)\tau}{2}\right)}{1 - \left(\frac{1 - r_1}{1 - r_2}\right)\exp\left(\frac{(r_2 - r_1)\tau}{2}\right)} \tag{25}$$

and

$$V(t) = \left(\frac{\theta - \Delta\Omega}{\theta}\right)\exp(-\theta\tau) + \frac{\Delta\Omega}{\theta} \tag{26}$$

where $r_1 = -\theta + (\theta^2 + 2\Omega)^{1/2}$ and $r_2 = -\theta - (\theta^2 + 2\Omega)^{1/2}$.

The numerical and asymptotic analytical solutions are shown in Fig. 7 for $\Delta = 0.01$, $\theta = 1.0$, and $\Omega = 1.0$. In this case only, equally spaced elements in w, not $\bar{D}$, were used because of the large number of particles generated in the small size range. A reason for the deviation in this range is because the asymptotic solution does not hold. $N(t)$ and $V(t)$ were computed from (25) and (26) and compared to the numerically computed values of N and V. The results are given in Table VI, where we see that, for the time considered, there is little finite domain error.

TABLE VI

Finite Domain Error for Case 6; $\beta_v = \beta_0$, $S_v = (S_0/v^*)\, e^{v/v^*} - R_0 n_v$[a]

τ[b]	$\frac{N_{analytic}}{N_{numeric}}$	$\frac{V_{analytic}}{V_{numeric}}$
0.25	1.00	0.994
1.0	1.00	0.992
2.0	1.00	0.986

[a] $\Omega = S_0/N_0^2\beta_0 = 1.0$, $\theta = R_0/N_0\beta_0 = 1.0$, and $\Delta = v^*/v_0 = 0.01$.
[b] $\tau = N_0\beta_0 t$.

5. Summary

The principal alternatives to the method of weighted residuals for the solution of (1) either rely on assumptions on the expected shape of the solution [11, 15] or employ discretization of particle sizes [6, 8–10]. The former class of methods, while computationally attractive, requires some prior knowledge of the solution. For a

discrete or finite-difference solution to account for all possible particle sizes, the mesh spacing must, in principle, be equal to the size of the smallest particle. The number of particle sizes needed to represent exactly a distribution between particle volumes v_a and v_b is v_b/v_a ; for atmospheric aerosols this ratio can be 10^{10}. Clearly, for a discrete solution to be computationally feasible the mesh spacing must be several orders of magnitude larger than the size of the smallest particle. In such a case substantial errors may be committed when representing the integral terms in (1). For problems of the type considered here methods of weighted residuals, such as collocation on finite elements, appear to be more attractive and efficient than finite-difference methods.

Although no definite conclusions can be made on which finite element technique is best for all cases, the advantages and disadvantages of each technique should be pointed out. For $\bar{M}$ collocation points cubic splines requires the solution of a $(\bar{M} - 2)$-dimensional tridiagonal linear system, while orthogonal collocation on finite elements requires the solution to a linear system with a banded matrix of bandwith 7. However to evaluate the distribution, orthongonal collocation on finite elements is considerable easier. The major difference between the two techniques is the location of the collocation points relative to the grid points. Orthogonal collocation on finite elements has the flexibility of locating the collocation points anywhere within the element (although the roots of an orthogonal polynomial are considered optimal). In cubic splines the collocation points are fixed at the grid points, but twice as many elements can be used for the same number of collocation points and the fit has continuous second derivatives.

The major source of error in solving (1) by collocation on finite elements is the use of a finite computational domain. The cases considered here represent a severe test of the so-called finite domain error because the distributions for those cases for which analytical solutions can be obtained tend to have uncharacteristically large numbers of particles at the upper end of the size spectrum when compared with most actual particulate systems. For most actual particulate systems the range of particle sizes is finite, and the finite domain error can be expected to be considerably less than that for cases such as those considered here. Hence time integrations can be performed for a longer time span.

ACKNOWLEDGMENT

This work was supported by Environmental Protection Agency contract 68-02-2216 and by National Science Foundation grant ENV76-04179.

REFERENCES

1. R. L. DRAKE, "Topics in Current Aerosol Research" (G. Hidy and J. Brock, Eds.), Pergamon, Oxford, 1972.
2. T. E. RAMABHADRAN, T. W. PETERSON, AND J. H. SEINFELD, *AIChE J.* **22** (1976), 840.
3. A. M. GOLOVIN, *Soviet Phys. Doklady* **8** (1963), 191.

4. W. T. Scott, *J. Atmospheric Sci.* **25** (1968), 54.
5. T. W. Peterson, F. Gelbard, and J. H. Seinfeld, *J. Colloid Interface Sci.* **63** (1978), 426.
6. G. M. Hidy, *J. Colloid Sci.* **20** (1965), 123.
7. S. Twomey, *J. Atmospheric Sci.* **23** (1966), 405.
8. L. F. Mockros, J. E. Quon, and A. T. Hjelmfelt, *J. Colloid Interface Sci.* **23** (1967), 90.
9. K. Takahashi and M. Kasahara, *Atmospheric Environment* **2** (1968), 441.
10. A. Suzuki, N. F. H. Ho, and W. I. Higuchi, *J. Colloid Interface Sci.* **29** (1969), 552.
11. E. R. Cohen and E. U. Vaughan, *J. Colloid Interface Sci.* **35** (1971), 612.
12. D. A. Gillette, *Atmospheric Environment* **6** (1972), 451.
13. E. X. Berry, *J. Atmospheric Sci.* **24** (1967), 688.
14. J. W. Burgmeier, I. H. Blifford, and D. A. Gillette, *Water, Air and Soil Pollution* **2** (1973), 97.
15. P. N. Singh and D. Ramkrishna, *J. Colloid Interface Sci.* **53** (1975), 214.
16. P. Middleton and J. Brock, *J. Colloid Interface Sci.* **54** (1976), 249.
17. B. A. Finlayson, "The Method of Weighted Residuals and Variational Principles," Academic Press, New York, 1972.
18. J. V. Villadsen and W. E. Stewart, *Chemical Engineering Sci.* **22** (1967), 1483.
19. H. C. Martin and G. F. Carey, "Introduction to Finite Element Analysis," McGraw–Hill, New York, 1973.
20. G. F. Carey and B. A. Finlayson, *Chemical Engineering Sci.* **30** (1975), 587.
21. G. Dahlquist and A. Biorck, "Numerical Methods," Prentice–Hall, Englewood Cliffs, N.J., 1974.
22. B. Carnahan, H. A. Luther, and J. O. Wilkes, "Applied Numerical Methods," Wiley, New York, 1969.